Optica Applicata, Vol. LV, No. 2, 2025
DOI: 10.37190/oa/202342

Optical fiber accelerometer for shock motion measurement

VAN-QUYET NGUYEN[1,2], CHIA-CHIN CHIANG[1], HSIANG-CHENG HSU[3], LIREN TSAI[1,*]

[1] Department of Mechanical Engineering, National Kaohsiung University of Science and Technology, No. 415, Jiangong Rd., Sanmin Dist., Kaohsiung City 807618, Taiwan

[2] Faculty of Mechanical Engineering, Nha Trang University, No. 02 Nguyen Dinh Chieu Street, Nha Trang City, Khanh Hoa 57000, Vietnam

[3] Department of Ph.D. Program in Maritime Science and Technology, National Kaohsiung University of Science and Technology, Kaohsiung 805301, Taiwan

[*] Corresponding authors: liren@nkust.edu.tw

This study proposes an accelerometer to measure shock motion with a fiber Bragg grating (FBG) sensing element attached to a 3D-printed elastomer structure. The structure is designed to be able to measure shock motion from two directions ($+X$ and $-X$) in 1D space using two optical sensors, FBG1 and FBG2, respectively. The deformation in the elastic structure leads to a change in the wavelength of the sensing element, and it is observed that the total Bragg wavelength shifts over the recorded acceleration range are 2.42 nm (FBG1) and 1.40 nm (FBG2) with a randomly generated acceleration between zero g and $600g$ ($1g = 9.81$ m/s^2). Numerical simulations are also used to observe the suitable working frequency range for the proposed accelerometer and the suggested working frequency range for this sensor in the range of 40–240 Hz. Such sensors are typically used in impact testing, safety validation, and heavy industrial applications, where the magnitude of acceleration is extremely high but the frequency content remains relatively low.

Keywords: shock accelerometers, acceleration sensors, fiber Bragg gratings, motion measurement, 3D-printed structure.

1. Introduction

Fiber Bragg grating (FBG) sensor has many outstanding advantages, such as anti-electromagnetic interference, anti-corrosion, small weight, unaffected by light source intensity, and powerful multiplexing capabilities. Therefore, FBG has been studied and applied a lot in recent years. FBG-based sensors have been extensively studied in recent years. It is widely applied in measuring technical parameters such as pressure, temperature, humidity, liquid level, acceleration, and even detecting chemical compositions and leaks [1-7].

In the field of accelerometers today, piezoelectric accelerometers are being used a lot because of their advantages, such as neat design, variety of types, easy use and simple operation. Besides the mentioned advantages, they also suffer from linearity problems and limited accuracy due to the influence of ambient noise and piezoelectric materials [8,9]. Capacitive accelerometers are also highly sensitive and can have extremely small frequency responses and wide ranges. However, their biggest disadvantage is that they are very susceptible to signal noise caused by the external environment. Therefore, they are only suitable for low-frequency fields, such as geological exploration or seismic detection [10].

Regarding the FBG accelerometer, recent research has also focused on developing and applying them to engineering measurements, from accelerometers applied in one -dimensional space to two-dimensional and three-dimensional with many different structures and materials used [11]. However, many studies have focused on low and medium frequency ranges with accelerations of only about one g (acceleration due to gravity on earth is $g = 9.81$ m/s^2) or a few g for slow and medium motions [12-15]. Meanwhile, high-speed shock motion mainly uses piezoelectric accelerometers and rarely uses FBG sensors [16]. In a previous study, FBG accelerometer sensors in one-dimensional space were also studied a lot but focused on one direction, meaning they can only measure the acceleration generated in the $+X$-direction [17]. However, they cannot measure if there is an acceleration in the opposite direction ($-X$).

Over the years and in the future, 3D printing technology has developed rapidly and contributed a lot of value to science, technology, and production. In the field of sensors, this technology is used as a facilitator to fabricate the structure for the sensor. The 3D printing technology excels in easy customization, automatic operation, and low production costs. In this study, the authors propose an accelerometer based on an FBG sensor attached to a 3D-printed elastic structure that can measure shock motion with accelerations ranging from zero g to $600g$ in both $+X$ and $-X$ directions.

2. Sensor description

2.1. Working principle

The centre of the Bragg wavelength is called λ_B, and it depends on the following two parameters:

$$\lambda_B = 2 n_{eff} \Lambda \tag{1}$$

where n_{eff} denote the effective refractive index of the core, and Λ is the periodicity of the grating.

The shift of the Bragg wavelength, denoted as $\Delta\lambda_B$, is determined by alterations in n_{eff} and Λ. These alterations are primarily influenced by the axial strain $\Delta\varepsilon$ and the temperature of the operating environment ΔT. Consequently, the variation in Bragg wavelength due to changes in strain and temperature can be mathematically represented by the following equation [18,19]:

$$\frac{\Delta\lambda_B}{\lambda_B} = (1 - p_e)\Delta\varepsilon + (a_f + \xi)\Delta T \tag{2}$$

where p_e is the elasto-optical coefficient, a_f is the thermal expansion coefficient, and ξ is the thermal optic coefficient.

The proposed FBG sensor has an elastic structure, and two FBGs are fixed to the structure so that it is sensitive to the effects of shock movements. When shock motion is generated, the sensitive structure of the accelerometer will be impacted to deform the grating inside the FBG, resulting in a change in the Bragg wavelength peak recorded by the IMON system. Additionally, the experiment was conducted within a controlled laboratory setting and under standard room temperature conditions, ensuring that any potential impact from room temperature can be negligible.

2.2. Sensor structure

The sensor structure is designed by SOLIDWORKS software and then simulated by ANSYS software to observe its behaviour. After that, the structural design is transferred to UltiMaker Cura software to set parameters before printing. Next, the 3D printer – INFINITY X1E was used to print the texture with an elastomeric polylactic acid (PLA) material, which has basic parameters such as a density of 1290 kg/cm^3, a Poisson ratio of 0.35 and Young's modulus is 3.45 GPa.

The 3D printer is operated with some basic parameters as follows: layer thickness (0.15 mm), fill density (100%), travel speed (60 mm/s), bed temperature (65 °C), and printhead temperature (220 °C). The whole process from design to completion of the structure, is shown in Fig. 1. The weights of the two mass blocks on opposite sides are designed to be equal. The overall dimensions of the sensor structure after 3D printing are L = 55 mm, W = 15 mm, H = 38 mm, which are length, width, height respectively.

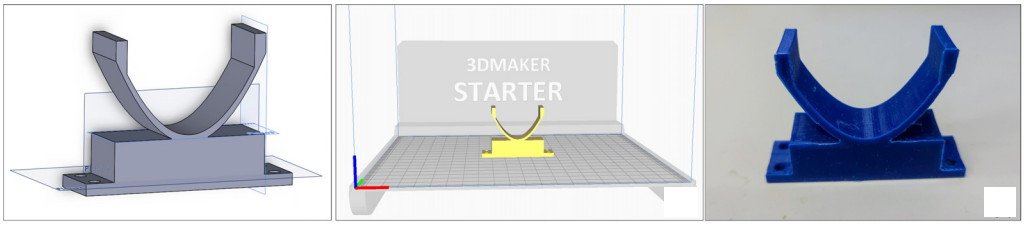

Fig. 1. Sensor structure. (a) Structural design, (b) the structure imported to UltiMaker Cura software before printing, and (c) the structure after 3D printing.

2.3. Packaged and connection

After the 3D printed structure is completed, two sensors, FBG1 and FBG2, are attached to the structure, as shown in Fig. 2. The two ends of FBG1 and FBG2 are fixed to the structure by the MXBON superglue made in Taiwan. Then, the whole structure including FBGs is connected to the Hopkinson bar system for experimental preparation.

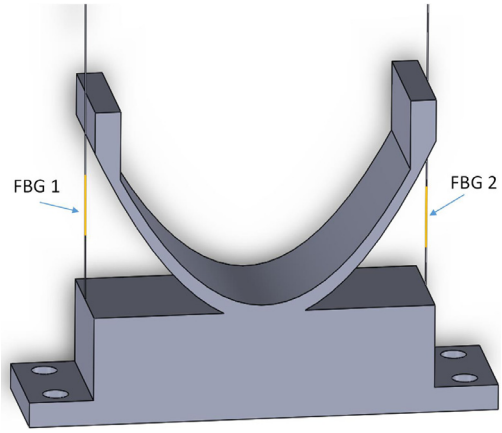

Fig. 2. Packaged sensor.

The Hopkinson bar system is a system that can dynamically test shock movements at high speed, and it was chosen to test the proposed sensor's performance.

2.4. Experiment setup

The experimental setup for the proposed FBG acceleration test is illustrated in Fig. 3. A 3D-printed base plate connects the accelerometer assembly to the Hopkinson bar's rod end. A piezoelectric accelerometer (PCB-305D2) is secured to the fixture's bracket. Light from a diode laser (DL-BP1-CS5169A) is coupled to the FBG via an optical coupler, with the reflected spectrum analyzed by an I-MON E-USB 2.0 interrogator. Signal acquisition and processing are performed using dedicated software. The laboratory temperature was maintained at 25 °C ± 0.5 °C to minimize thermal effects.

The sensor is tested under $\pm X$ accelerations on the Hopkinson bar in turn. The random acceleration is generated by a pneumatic chamber controlled to act on the Hopkinson

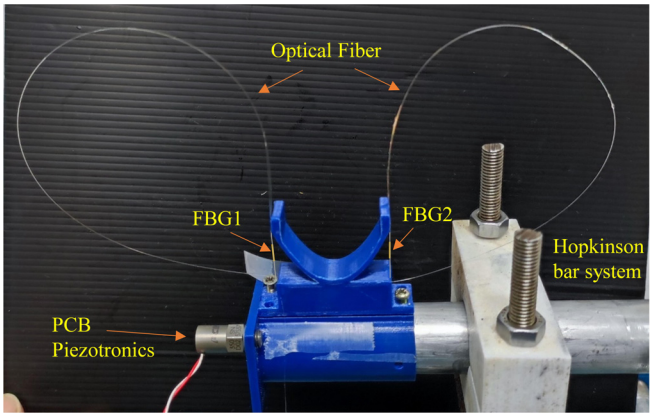

Fig. 3. Experiment set-up.

bar. The dynamic load induced strain variations in the fiber, causing Bragg wavelength shifts recorded by the IMON. A pulse accelerometer (PCB-350D2) connected to a DAQ-NI9234 and LabVIEW software provided comparative acceleration measurements, consistent across both directions.

3. Result and discussion

After performing experiments as well as numerical simulation, some results were obtained as follows.

3.1. Shock response

Figures 4 and 5 show the signals obtained during the acceleration test with the Hopkinson bar system. When the accelerometer appears on the Hopkinson bar, which is recorded

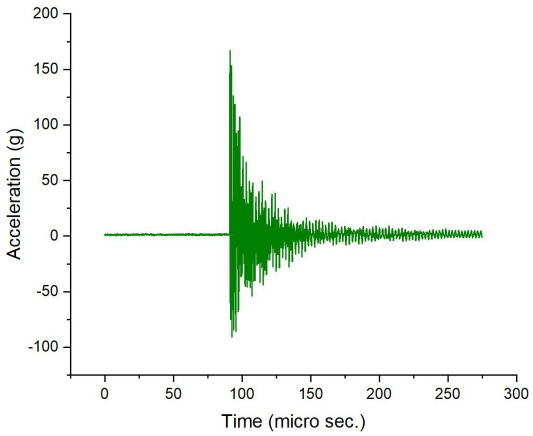

Fig. 4. Acceleration signals obtained from DAQ system.

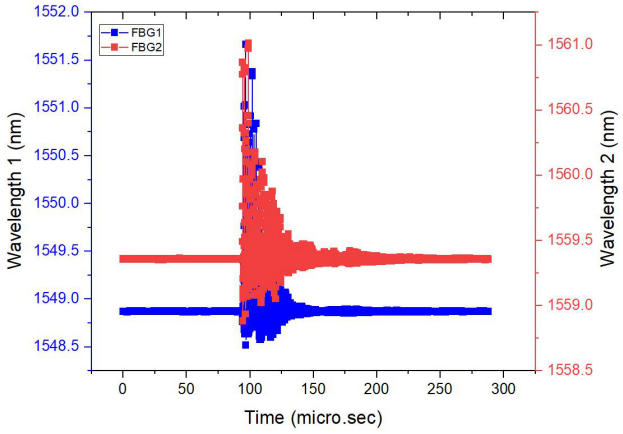

Fig. 5. Wavelength signals obtained from IMON system.

by the DAQ system, it causes the elastic structure of the sensor to respond in the direction opposite to the direction of the acceleration, from which the sensors FBG1 and FBG2 will receive the signals. The wavelength signals inside the fiber sensor are recorded from the IMON system.

3.2. Sensor performances

The obtained results show that when the acceleration is randomly generated in the range of 0–600 *g*, the signal recorded from the FBG sensor to the IMON system is compatible with the change in acceleration. This means that as the acceleration increases, the wavelength peak change also increases, and as the acceleration decreases, the wavelength peak decreases accordingly (Fig. 6).

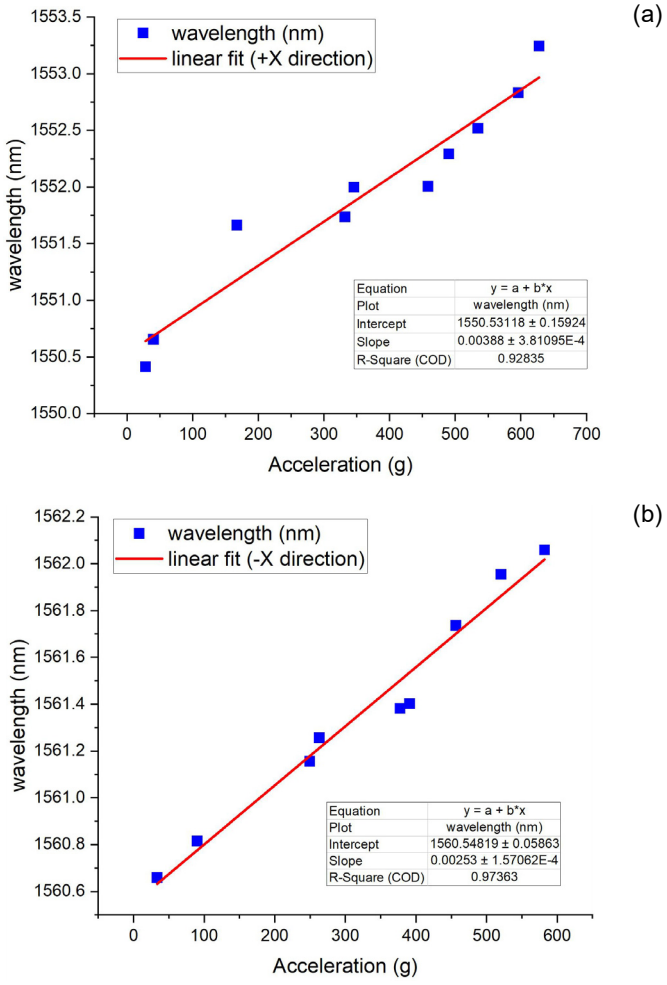

Fig. 6. The wavelength peak change corresponds to the acceleration change: the result obtained from (a) FBG1 and (b) FBG2.

Figure 6 shows that the total wavelength shift from FBG1 is 2.42 nm over the applicable acceleration range from 27.9g to 596.1g, corresponding to an accelerometer sensitivity of 3.88 pm/g. In FBG2, the total wavelength shift obtained is 1.40 nm over the applicable acceleration range of 33.4g to 582.1g, corresponding to an accelerometer sensitivity of 2.53 pm/g. The linear analysis results show that the linearity of the data obtained in the experiment is close to 93% for FBG1 and over 97% for FBG2. That means the stability during the working of the sensor is quite good. It is essential to highlight that the sensor's sensitivity decreases with increased test acceleration, rendering it inappropriate to make sensitivity comparisons within the low acceleration range of just a few g. Consequently, the authors abstain from providing commentary on sensitivity within this section, as it would be unfair to compare sensitivity (pm/g) under these circumstances. Some other studies also use Hopkinson rods to generate shock accelerometers but use piezoelectric accelerometers or strain gauges [20-22].

3.3. Harmonic response

The amplitude-frequency characteristic of the proposed sensor is simulated in the working environment of ANSYS with the Harmonic Respond module. The amplitude of the applied acceleration was kept constant at 600g, and the excitation frequency varied between 0 and 800 Hz with a step length of 40 Hz, as shown in Fig. 7. It also indicates that the recommended linear operating frequency of the FBG accelerometer is 40–240 Hz and the natural frequency is 400 Hz.

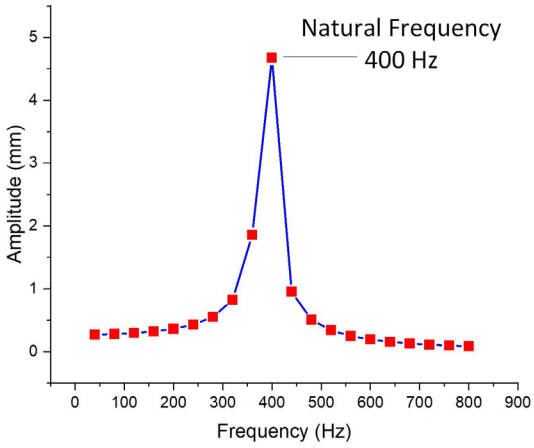

Fig. 7. Sensor working frequency range.

3.4. Customizability of the sensor

Figure 8 illustrates the alterations in deformation occurring within the FBG sensor as the mass weight undergoes variations. Because the weights of the two initial mass blocks are the same, the authors only analyze one side as an example here. Specifically, let the initial weight of the mass block be denoted as M (in grams), with subsequent

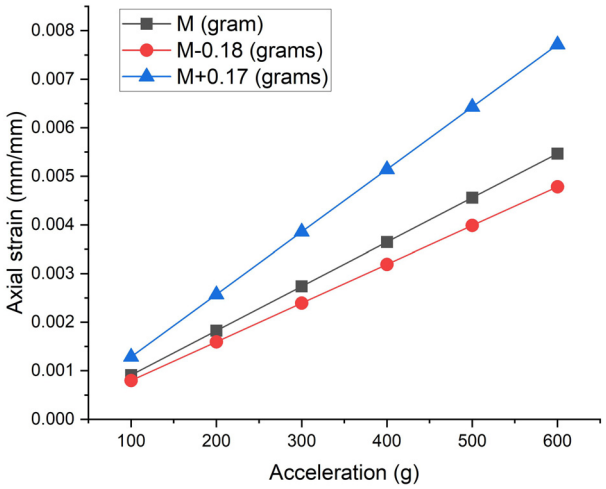

Fig. 8. Sensor response (axial strain) when mass block M changes.

weights designated as (M – 0.18) grams following a reduction and (M + 0.17) grams following an increase. The acceleration applicable to all three cases selected for analysis is from 100g to 600g.

Figure 8 also shows that with the same applied acceleration value if the weight of the mass block is increased, the axial strain occurring in the FBG sensor will also increase and *vice versa*. Specifically, with this sensor structure, when increasing the weight of mass to 0.17 grams, the axial strain increases 3.16 times, and if the weight of mass decreases by 0.18 grams, the axial strain decreases 1.14 times. Thus, it further demonstrates that a simple adjustment of the mass block's weight adapts this sensor to a higher or lower acceleration range. Moreover, the process becomes notably streamlined when utilizing 3D printing technology to fabricate the sensor's structure. The remarkable advantage of this technology lies in its high degree of customization, facilitating such modifications effortlessly.

3.5. Optimal conditions

Based on the results and analytical data presented above, for the sensor to operate stably and effectively, it is necessary to pay attention to some optimal conditions as follows:

1) Operate within the recommended frequency range (40–240 Hz) to ensure sensor linearity.
2) Control environmental temperature to minimize its effect on measurements.
3) Customize the "mass block" to suit the target acceleration range.
4) Note that the sensor's sensitivity may vary with acceleration, and therefore, consider calibration for specific acceleration ranges.

By considering these factors, the performance and reliability of the FBG accelerometer in shock motion measurement applications can be optimized.

4. Conclusion

This study tested the FBG accelerometer under shock motion generated from the Hopkinson rod system. The shock motion is randomly generated between zero *g* and 600*g* accelerations from two directions to evaluate the sensor's sensitivity, linearity, and stability. We observe that when the acceleration is changed randomly, the wavelength peak in the FBGs also changes accordingly; that is, as the acceleration increases, the wavelength shift also increases, and *vice versa*. Numerical simulations are also used to observe the suitable working frequency range for the proposed FBG accelerometer, and the proposed working frequency range for this sensor is suitable between 40–240 Hz, in the low-frequency range.

The proposed accelerometer has a structure printed with an elastic material (PLA) by 3D printing technology, so it has many advantages from the outstanding advantages of this technology, such as fast fabrication time, production cost savings, and especially easy customization. From the above highlights, this proposed acceleration methodology has great potential for application in related engineering fields; it enables manufacturers to customize 3D-printed structures, modulating the applied acceleration range for diverse applications. Such sensors are suitable for crash tests, safety validation, and machinery monitoring in heavy industries (*e.g.*, safety monitoring in drive systems and HVAC systems). For instance, it can be applied to evaluate the structural response of equipment under strong mechanical shocks, vibrations during transportation, or emergency shutdown scenarios, thereby ensuring the safety of machines, equipment, and human operators following engineering safety standards.

Acknowledgements
This work was supported by the Ministry of Science and Technology, Taiwan, under Grant MOST 112 -2221-E-992-077- and Nha Trang University for science and technology under grant no. TR2024-13-27.

References

[1] Vorathin E., Hafizi Z.M., Ismail N., Loman M., *Review of high sensitivity fibre-optic pressure sensors for low pressure sensing*, Optics and Laser Technology **121**, 2020: 105841. https://doi.org/10.1016/j.optlastec.2019.105841

[2] Huang J., Zhou Z., Zhang D., Wei Q., *A fiber Bragg grating pressure sensor and its application to pipeline leakage detection*, Advances in Mechanical Engineering **5**, 2013: 590451. https://doi.org/10.1155/2013/590451

[3] Bedi A., Kothari V., Kumar S., *Design and analysis of FBG based sensor for detection of damage in oil and gas pipelines for safety of marine life*, Proceedings of the SPIE, Vol. 10488, Optical Fibers and Sensors for Medical Diagnostics and Treatment Applications XVIII, 2018: 104880X. https://doi.org/10.1117/12.2285923

[4] Nguyen V.Q., Chiang C.-C., Tsai L., *Enhanced sensitivity of bare FBG pressure sensor based on oval-shaped 3D printed structure*, Optical Fiber Technology **73**, 2022: 103022. https://doi.org/10.1016/j.yofte.2022.103022

[5] Nguyen V.Q., Chiang C.-C., Tsai L., *Simple pressure sensor with highly customizable sensitivity based on fiber Bragg grating and pill-shaped 3D-printed structure*, Journal of Sensors, Vol. 2022, 2022: 9248873. https://doi.org/10.1155/2022/9248873

[6] LIN Y.-K., HSIEH T.-S., TSAI L., WANG S.-H., CHIANG C.-C., *Using three-dimensional printing technology to produce a novel optical fiber Bragg grating pressure sensor*, Sensors and Materials **28**(5), 2016: 389-394.

[7] CHIANG J.-S., CHANG H.-Y., SUN N.-H., LIU W.-F., *High sensitive two-dimension tilted-meter based on chirped fiber Bragg gratings*, IEEE Sensors Journal **16**(23), 2016: 8477-8482. https://doi.org/10.1109/JSEN.2016.2582507

[8] SHIVASHANKAR P., GOPALAKRISHNAN S., *Review on the use of piezoelectric materials for active vibration, noise, and flow control*, Smart Materials and Structures **29**(5), 2020: 053001. https://doi.org/10.1088/1361-665X/ab7541

[9] PRAMANIK R., AROCKIARAJAN A., *Effective properties and nonlinearities in 1-3 piezocomposites: A comprehensive review*, Smart Materials and Structures **28**(10), 2019: 103001. https://doi.org/10.1088/1361-665X/ab350a

[10] D'ALESSANDRO A., SCUDERO S., VITALE G., *A review of the capacitive MEMS for seismology*, Sensors **19**(14), 2019: 3093. https://doi.org/10.3390/s19143093

[11] GUO Y., CHEN M., XIONG L., ZHOU X., LI C., *Fiber Bragg grating based acceleration sensors: A review*, Sensor Review **41**(1), 2021: 101-122. https://doi.org/10.1108/SR-10-2020-0243

[12] FAN W., WEN J., GAO H., QIAO X., *Low-frequency fiber Bragg grating accelerometer based on diaphragm-type cantilever*, Optical Fiber Technology **70**, 2022: 102888. https://doi.org/10.1016/j.yofte.2022.102888

[13] LI H., ZHANG X., ZHOU R., QIAO X., *Low frequency fiber optic accelerometer based on lever amplification structure*, Optical Fiber Technology **80**, 2023: 103434. https://doi.org/10.1016/j.yofte.2023.103434

[14] XU Y., FAN W., GAO H., QIAO X., *Fiber Bragg grating low-frequency accelerometer based on spring structure*, Optical Fiber Technology **82**, 2024: 103614. https://doi.org/10.1016/j.yofte.2023.103614

[15] GUO T., SONG H., SHA S., LI C., XU M., *Highly sensitive fiber bragg grating accelerometer with low resonant frequency*, Optical Fiber Technology **87**, 2024: 103919. https://doi.org/10.1016/j.yofte.2024.103919

[16] NGUYE V.-Q., CHIANG C.-C., HSU H.-C., TSAI L., *Shock accelerometer based on fiber Bragg grating sensor with a novel 3D printed structure for medium frequency measurement applications and high acceleration range*, Optical Fiber Technology **80**, 2023: 103386. https://doi.org/10.1016/j.yofte.2023.103386

[17] NGUYEN V.Q., CHIANG C.-C., LE H.-D., TSAI L., *Fabrication and testing of FBG sensor-based one-dimensional shock accelerometer attached to novel 3D printed structure*, Optik **276**, 2023: 170632. https://doi.org/10.1016/j.ijleo.2023.170632

[18] WANG X., GUO Y., XIONG L., WU H., *High-frequency optical fiber Bragg grating accelerometer*, IEEE Sensors Journal **18**(12), 2018: 4954-4960. https://doi.org/10.1109/JSEN.2018.2833885

[19] HISHAM H., *Fiber Bragg Grating Sensors: Development and Applications*, CRC Press 2019.

[20] FOSTER J.T., FREW D.J., FORRESTAL M.J., NISHIDA E.E., CHEN W., *Shock testing accelerometers with a Hopkinson pressure bar*, International Journal of Impact Engineering **46**, 2012: 56-61. https://doi.org/10.1016/j.ijimpeng.2012.02.006

[21] FREW D.J., DUONG H., *A modified Hopkinson pressure bar experiment to evaluate a damped piezoresistive MEMS accelerometer*, Proceedings of the SEM Annual Conference, Albuquerque, New Mexico, USA, 2009.

[22] FORRESTAL M.J., TOGAMI T.C., BAKER W.E., FREW D.J., *Performance evaluation of accelerometers used for penetration experiments*, Experimental Mechanics **43**, 2003: 90-96. https://doi.org/10.1007/BF02410489

Received December 28, 2024
in revised form February 5, 2025